12-2019

In Vivo Metabolic and Vascular Response to Hypoxia in Twist Knockdown Murine Breast Cancer

Brandon Sturgill
University of Arkansas, Fayetteville

In Vivo Metabolic and Vascular Response to Hypoxia in Twist Knockdown Murine Breast Cancer

A thesis submitted in partial fulfillment
of the requirements for the degree of
Master of Science in Biomedical Engineering

by

Brandon Sturgill
Oklahoma Baptist University
Bachelor of Science in Physics, 2016

December 2019
Univeristy of Arkansas

This thesis is approved for recommendation to the Graduate Council.

_____
Narasimhan Rajaram, Ph.D.
Thesis Director

_____
Kyle Quinn, Ph.D.
Committee Member

_____
Timothy Muldoon, Ph.D.
Committee Member

Abstract

Twist transcription factor is often overexpressed in aggressive tumors. Although needed in early embryonic development for organogenesis, Twist is known to induce an epithelial to mesenchymal transition in cells. In cancer, epithelial to mesenchymal transitions can lead to increased motility and invasiveness. It has also been linked to metabolic reprogramming and increased metastatic risk. Furthermore, metabolic preferences can increase proliferation, enhance metastatic potential, and influence the site of metastasis. We hypothesize that Twist directly affects the metabolism of cancer cells. We expect to see *in vivo* what we have seen *in vitro*; Twist overexpression should promote a shift away from glycolysis in response to reperfusion.

To study the effects of Twist on metabolism *in vivo* tumors were grown in the dorsal skinfold window chamber and stressed by exposure to hypoxia. Knowledge of metabolism without information on the oxygen availability is incomplete because cell metabolism naturally shifts between oxidative phosphorylation and glycolysis in response to variations in oxygen availability. Knowing if oxygen is readily available is particularly important when studying cancer metabolism because tumors may have poor vasculature organization due to angiogenesis not keeping up with tumor growth. To know if metabolic changes are due to intrinsic or extrinsic factors hyperspectral imaging was used to determine vascular oxygenation within the tumor. Multiphoton microscopy was used to quantify metabolism on the cellular level by measuring the optical redox ratio as well as the relative contribution ratio of free and bound NADH.

We found the optical redox ratio, vascular oxygenation, and hemoglobin concentration were affected more by hypoxia in the cell line not expressing Twist. This would suggest that Twist does have a direct impact on metabolism within the cell. Because multiphoton imaging was not performed during hypoxia, whether Twist causes quicker metabolic changes or causes resistance to metabolic change remains to be determined.

Table of Contents

1. Introduction

1.1 *Twist and metabolism*

There are clear changes that occur in tissue as it transitions from normal to cancerous. These changes range from morphologic to metabolic.[1] However, the differences between metastatic tumors and nonmetastatic tumors are more subtle. Metastasis is a multistep process and the ability to complete one step of that process does not guarantee metastasis has or will occur, and if unique hallmarks of metastasis can be identified it may provide a way to avoid unnecessary, life changing therapies for nonmetastatic tumors.[2]. The gene TWIST encodes for a transcription factor which is associated with metastatic potential.[3,4] By comparing a Twist-positive, metastatic murine breast cancer cell line to the same cell line with Twist expression knocked down we aim to determine if there are phenotypic changes in the microenvironment or metabolism associated with metastasis.

The transcription factor Twist, when expressed properly, is critical to biological functions such as embryonic development and organogenesis.[3,5] However, when overexpressed in cancers Twist is associated with increased metastatic potential and poor long term outcome.[3,5,6] Twist may promote metastasis by inducing epithelial to mesenchymal transition (EMT) or energy metabolism reprogramming (EMR) which have been linked to increased proliferation, invasiveness, and cell survival.[3,7,8]

The reprogramming of cancer metabolism was proposed first by Otto Warburg when he discovered cancer cells prefer glycolysis in the presence of adequate oxygen.[9] Glycolysis is typically a way for cells to continue production of adenine triphosphate (ATP) during hypoxia. However, in proliferating cancer cells aerobic glycolysis may instead be utilized to support rapid, uncontrolled proliferation by increasing glucose metabolism to generate nutrients needed for rapid cell division.[10]

It is important to note that even under aerobic glycolysis there is adequate ATP production even though glycolysis has a much lower yield of ATP than oxidative phosphorylation (OXPHOS). Aerobic glycolysis and OXPHOS may be used in tandem to increase the rate of ATP production.[11] The increased rate of glycolysis is not necessarily done to increase ATP production since many cell lines continue producing the majority of their ATP through OXPOHOS even when glycolysis has increased.[12] Evidence suggests the primary function of aerobic glycolysis in most proliferating cells is not an alternative means of ATP production, but rather a method of synthesizing molecules required in cell proliferation.[13]

Metabolic alterations can have a significant impact on tumorigenicity and metastatic potential. Lu et al found that tumorigenicity and metastatic ability is gained in a two-step metabolism altering process.[14] Formation in the primary tumor shows changes in glycolysis, the pentose phosphate pathway, and fatty acid synthesis; further change in glycolysis, the TCA cycle, and nucleotide metabolism occurs during metastasis.[14] Utilization of OXPHOS has been shown to increase metastatic potential in murine breast carcinoma whereas the repression of mitochondrial respiration limited cell motility.[15,16] Although increased use of OXPHOS may lead to a more metastatic phenotype, tumors consist of a largely heterogenous cell population, and within the heterogenous tumor, a cell's metabolic phenotype can determine its site of metastasis.[17] It is clear that metabolic adaptations can provide distinct advantages to cells during proliferation, invasion, and at metastatic sites.

Twist can affect tumor progression in many ways; such as inhibition of p-53 activated cell apoptosis, promotion of cell motility and tumor invasiveness through EMT, and inducing EMR.[3,7,18] The metabolic phenotype as altered by Twist overexpression has also been shown to affect tumor invasiveness and metastatic ability.[3,4,6,7,18,19] One important factor found *in vivo* is the tumor vasculature. The high proliferation rate of tumors can outpace angiogenesis and lead to local hypoxia, which in turn leads to the release of angiogenic factors. The resulting tumor

vasculature may be poorly organized, leaky, and provide inconsistent blood flow.[20] Therefore, observations made in cell culture or organoids should be tested *in vivo* to determine the effects of Twist on cell metabolism within the more complex environment of living tissue. Intravital microscopy provides a way to study these vascular and metabolic changes.

1.2 *Advantages of the dorsal skinfold window chamber*

The dorsal skinfold window chamber can be used in conjunction with intravital microcopy to observe metabolism and vascular oxygenation *in vivo*. The window chamber exposes the tumor within its microenvironment and allows for high resolution imaging of the tumor for up to two weeks.[21] The noninvasive nature of optical imaging with the window chamber allows for longitudinal studies of the early tumor and its natural environment.[21,22] Imaging utilizing exogenous contrast agents, endogenous fluorophores, and absorbance by molecules such as hemoglobin can be used to measure metabolic and vasculature characteristics of the tumor microenvironment.[21–25]

The window chamber has been used with fluorescent glucose analog 2-NBDG to determine glucose uptake in cancer cell lines with different metastatic potentials. In addition to glucose uptake, vascular oxygenation was determined with hyperspectral imaging, and together they were used to quantify aerobic glycolysis.[24] This elucidates the amount of glucose being used and oxygen availability, but does not provide metabolic information on a cellular level.

1.3 *Multiphoton imaging: optical redox ratio and fluorescent lifetime imaging*

Multiphoton microscopy (MPM) can be used to investigate metabolic changes on the cellular level. MPM is in many ways similar to traditional confocal fluorescent microscopy. In both fluorophores are excited by incident light and the resulting emission is recorded, and both have the advantage of reducing noise from outside the focal plane. The primary difference between the two imaging methods is the excitation source. Where traditional fluorescence

microscopy uses high energy, short wavelength photons to excite fluorophores MPM uses lower energy, longer wavelength photons. Traditionally only a single photon needs to be absorbed to cause fluorescence, but in MPM two photons with half the wavelength are absorbed simultaneously. This provides MPM with multiple benefits. Longer wavelengths of light can travel further in tissue before being absorbed which allows for a greater imaging depth, and since these wavelengths are typically longer than ultraviolet light they cause less cellular damage and photo bleaching. Additionally, since the simultaneous absorption of two photons is a rare event only fluorophores close to the plane of focus are excited. This reduces noise from fluorescence in surrounding tissue.

The benefits of multiphoton microscopy make it especially useful for *in vivo* imaging. For years it has been used to measure metabolism in cells by excitation of endogenous fluorophores.[26] Nicotinamide adenine dinucleotide (NADH) and flavin adenine dinucleotide (FAD) are fluorescent metabolic cofactors, although only the reduced form of NADH and oxidized form of FAD are fluorescent. The optical redox ratio (ORR) is defined here as FAD/NADH+FAD and changes in the ORR have been associated with changes in metabolic activity.[15,26,27] $FADH_2$ is reduced to FAD (fluorescent) and NADH is oxidized to NAD (nonfluorescent) during OXPHOS leading to the an increase in the ORR. During glycolysis mitochondrial activity is expected to decrease which leads to a buildup of NADH and a decrease of the ORR. There is evidence for the relationship between the ORR and glycolysis in a study showing strong correlation between the ORR and oxygen consumption rate when compared to results from seahorse flux analyzers (Seahorse XF^e24 and Seahorse XFp).[15,28] The ORR is not an exact measurement of glycolysis and OXPHOS, but rather the relative use of the two.

Additionally, fluorescent lifetime imaging (FLIM) can be used to probe metabolism. Instead of recording the fluorescent intensity as is done is for the ORR, FLIM records the amount of time fluorophores remain in the excited state. Of particular interest is NADH. Lifetime

of NADH is primarily affected by whether it is bound to a protein. The lifetime is many times longer when bound than when free.[29,30] Lifetime and relative contribution of free and bound NADH are computed by fitting each pixel from the FLIM image to a biexponential decay model.[29] Although the primary cause of differences in lifetime is determined by whether NADH is free or bound other factors can affect it as well. Factors within the microenvironment such as pH, temperature, and oxygen concentration can affect the lifetimes to a lesser extent.[31] The bound lifetime of NADH is also sensitive to the metabolic pathways being used.[32]

The relative ratio of free to bound NADH (A1/A2) can also indicate prevalence of glycolysis or OXPHOS, with an increasing A1/A2 ratio being indictive of increased glycolysis or decreased OXPOHS.[33,34] As relative use of glycolysis increases and OXPHOS decreases there is a buildup of NADH. This NADH when not undergoing oxidation/reduction reactions will be bound to proteins less often than when it's being actively used in the electron transport chain or other metabolic processes. The lack of binding means an increase in the relative amount of free NADH (A1) which increase the A1/A2 ratio.

In vitro models are indispensable tools, but have been shown to miss effects of the tumor microenvironment which can affect metabolism.[35] Tumor vasculature is critical to the native tumor environment. Poorly organized vasculature, caused by rapid proliferation and angiogenesis, can lead to poor blood flow, local hypoxia, and decreased nutrient transport.[20] Furthermore, glycolysis is a naturally occurring adaptation to hypoxia. So, it must be determined whether metabolic changes *in vivo* are caused by somatic changes in the cells or by oxygen availability. Hyperspectral imaging can be used for this purpose.

1.4 *Hyperspectral imaging*

Hyperspectral imaging of hemoglobin absorption can be used to determine shifts in oxygen content in tumor vasculature *in vivo*.[23–25] This imaging technique combines spectroscopy

and microscopy to create a spatial image that also carries spectral. In spectroscopy, the amount of light absorbed when passing through a sample can be measured over many wavelengths. Absorptivity of a sample is wavelength dependent which allows characteristics that alter absorptivity to be quantified. Hyperspectral imaging uses this same technique but expands the spectrographic measurement to every pixel in an image. The absorption spectra at each pixel is used to determine the total hemoglobin and the vascular oxygenation by fitting the spectra to known functions. The spectral images can be gathered by combining an tunable band pass filter with bright field microscopy.[36]

Hyperspectral imaging has been used in a plethora of biomedical studies.[36] It is used to measure absorbance, reflection, and fluorescence.[23,36] Absorbance can only be used when tissue samples are thin enough for light transmission such as with the window chamber. This is possible because oxy-hemoglobin and deoxy-hemoglobin have different absorbance spectra and when mixed the relative contribution of each can be determined.[25] The oxygen saturation is generally important in cancer studies because- as discussed earlier- rapid proliferation can lead to local hypoxia and poorly developed vasculature within the tumor. Without knowing what the oxygen condition is within the tumor whether cancer cells have undergone EMR or are only reacting to local hypoxia cannot be known.

A previous study in our lab using a panel of sibling murine breast cancer cell lines demonstrated an association between metastatic potential and metabolic adaptations to hypoxia.[15] Because Twist has been shown to be responsible for promoting metastatic behavior in these cells, a Twist-deleted clonal population of the most metastatic of these cell lines – 4T1 – was used to investigate metabolic changes in response to hypoxia. Preliminary studies *in vitro* showed that the metabolic changes in the Twist-deleted cell line (Twist-KO) in response to hypoxia resembled that of the on-metastatic cell line.

The overall objective was to study the effects of Twist transcription factor on the metabolism of hypoxia stressed cancer cells *in vivo*. We used the murine breast cancer cell lines 4T1 and Twist-KO to grow tumors in a dorsal skinfold window chamber. We used hyperspectral imaging to visualize oxygen saturation within the tumor microenvironment and multiphoton microscopy to quantify metabolic changes. Twist expression is expected to promote a glycolytic phenotype.[7] As a cell line shifts to glycolysis we expect to see a decrease in the redox ratio and an increase in the vascular oxygenation when compared to a less glycolytic cell line. We found that Twist expressing cell lines experience less metabolic change between normoxia and reperfusion than their Twist-deleted counterpart. Additionally, we found vascular oxygenation appears to respond to shifts in metabolism as expected.

2. Methods

2.1 *Animal protocols*

Dorsal skinfold window chambers were installed on female Balb c/J mice after shaving and nairing the necessary area. Mice were anesthetized with an intraperitoneal injection of ketamine / xylazine (100uL) and kept on a water circulating heat pad for the duration of the surgery and until regaining consciousness. During the window chamber installation approximately 10k 4T1 or 30k 4T1-Twist KO cells were suspended in 10uL of PBS and injected under the fascicular layer of the exposed skin. The glass coverslip was then mounted. Mice were given subcutaneous injections of rimadyl (5 mg/kg) on the left or right flank immediately after surgery and approximately twelve hours after surgery. Tumors typically developed in five to seven days post installation and injection.

To perturb cells within the microenvironment mice were exposed to hypoxic conditions for one hour. For hyperspectral imaging mice were imaged under normoxia, hypoxia, and reperfusion. Multiphoton microscopy was only performed under normoxia and reperfusion.

Before imaging, mice were placed in an induction chamber and were anesthetized using isoflurane mixed with air (2-2.5% v/v). During imaging anesthesia was supplied via a nose cone at 1.25-1.5% v/v, and mice were seated on an adjustable temperature electric heating pad (Physitemp MTC-1) kept at a constant temperature of 37ºC**.**

Mice were considered normoxic if they did not have prior exposure to hypoxia during the imaging session. The air mixture used for normoxia and reperfusion imaging was 21% and 100% O_2 for hyperspectral and multiphoton microscopy respectively. Mice were exposed to hypoxia for one hour. After one hour of hypoxic exposure mice were either imaged for vascular oxygenation or were allowed to recover. For hypoxic imaging 10% oxygen was used during anesthesia. Mice were allowed to recover in their cages breathing room air for one hour which allows for reperfusion of the vasculature. After one hour of recovery reperfusion imaging was done.

Mice were imaged on two consecutive days. Hyperspectral imaging was completed the first day and multiphoton microscopy the second. This was done so oxygenation had ample time to settle back to its baseline value before performing normoxic imaging again. After imaging was complete mice were euthanized by carbon dioxide inhalation.

2.2 *Oxygen perturbation*

To induce hypoxia the mice- within their cage- were placed in a large, inflatable glove bag. A tube was connected from the 10% oxygen tank and the bag was slowly inflated. A second tube was run from the bag to a large beaker containing a shallow amount of water. The end of this tube was placed just below the surface of the water. This caused escaping gas from the hypoxia chamber to create bubbles which indicated the amount of gas being replaced in the chamber. This insured that a constant 10% O_2 was maintained in the chamber. After one hour of exposure the gas was shut off and mouse removed. As mentioned previously, for hyperspectral

imaging mice were immediately anesthetized with isoflurane mixed with 10% oxygen for hypoxic imaging and were allowed to recover after imaging was complete. For multiphoton imaging, mice were removed and placed back in their cages to recover for one hour before reperfusion imaging was done.

2.3 *Hyperspectral imaging*

Commercially available components were used for image acquisition. An Olympus IX81 inverted microscope was used with a Hamamatsu Orcaflash 4.0+ monochrome CMOS camera for capturing images, and a Varispec Cri liquid crystal tunable filter band pass filter was placed between the 4x objective and the camera. Images were captured from wavelengths of 520nm to 620nm in 10nm increments. Integration time was changed at each wavelength to prevent saturation of the image. This is necessary because transmission of light through tissue is dependent on wavelength as is output by the light source. Integration time and wavelengths were recorded for each image and calibration images with neutral density filters were acquired under the same conditions. A dark image was also captured to calibrate for noise from sources other than that transmitted through the window chamber.

The different absorption spectra of oxygenated and deoxygenated hemoglobin makes it possible to determine the amount of oxygenation saturation within blood vessels by hyperspectral imaging. Our acquired images are processed with a custom Matlab program that utilizes the differences in absorption spectra. This code fits the pixel intensities over the range of wavelengths to a modified Beer-Lambert law eq 1.[24]

$$A(\lambda) = \log\left(\frac{I_0}{I}\right) = L * [\ \varepsilon_{HbO_2}(\lambda) * [HbO_2]\ +\ \varepsilon_{dHb}(\lambda) * [dHb]\ + S] \quad (1)$$

Where A is the wavelength dependent absorption, I_o is the incident light determined from calibration images, I is the transmitted light determined by pixel intensity, L is path length of the light, $\varepsilon_{HbO2}(\lambda)$ and $\varepsilon_{dHb}(\lambda)$ are the wavelength extinction coefficients of oxy- and

deoxyhemoglobin , [HbO_2] and [dHb] are the concentrations of oxy- and deoxyhemoglobin, and S is a term to account for scattering.[23] The pixel intensities of the compiled images are fit to the function to determine total hemoglobin concentration ([HbO_2] +[dHb]) and oxygen saturation ([HbO_2] / [HbO_2+ dHb]). Total hemoglobin concentration is used to create a mask that excludes pixels that are not vasculature, and then pseudo color images are created to visualize hemoglobin concentration and oxygenation. Grayscale transmission images are used to manually select regions of interest that exclude vasculature outside the tumor area. Average total hemoglobin and hemoglobin oxygenation were determined by dividing the summation of either by the summation of pixels in the binary, tumor vasculature mask.

2.4 *Multiphoton imaging*

Fluorescent intensity images and fluorescent lifetime images (redox and FLIM) were acquired using a 20x, 1.0NA, water immersion objective, using a 2.49 digital magnification, on a Bruker Ultima Investigator laser scanning microscope using a Spectra Physics Ti:Sapphire laser.[37] NADH and FAD fluorescence was caused with excitation wavelengths of 855nm and 755nm respectively. All images acquired were initially processed based on methods published previously.[37] Fluorescence intensity from NADH and FAD were normalized based on laser power and PMT gain. FLIM images were processed using commercially available software SPCimage.[37]

Fluorescent intensity images and fluorescent lifetime images (redox and FLIM) were acquired using a 20x, 1.0NA, water immersion objective, using a 2.49 digital magnification, on a Bruker Ultima Investigator laser scanning microscope using a Spectra Physics Ti:Sapphire laser.35 NADH and FAD fluorescence was caused with excitation wavelengths of 855nm and 755nm respectively. All images were initially processed based on previously published methods.[37] Fluorescence intensity from NADH and FAD were normalized based on laser power and PMT gain.

FLIM images were acquired using a dwell time of 4.8 µs**.** An integration time of two minutes was used with an excitation wavelength of 755nm which corresponds to NADH. Images were processed using SPCImage 6.4. Images were spatially binned twice and had a total pixel photon count of at least 10,000 photons. Using a bi-exponential decay model (equation 2) data lifetime data was separated into its short and long lifetime contributions.[37] This biexponential fit is expressed in equation 2 where I is the resulting intensity in the image, α_1 and α_2 are the relative contributions of

$$I = \alpha_1 e^{\tau_1/t} + \alpha_2 e^{\tau_2/t} \quad (2)$$

free and bound NADH, τ_1 and τ_2 are the lifetimes of free and bound NADH, and t is the measured time of fluorescence. Our primary interest is the relative contributions since they may indicate a shift in metabolism. The ratio of relative contributions was determined on a pixel-wise basis of masked FLIM images. Intensity images of FLIM were used to create masks using Otsu's method as well. An example of the masking process is shown in figure S1 in the appendix.

Using processed fluorescent intensity images masks were created to exclude non-cell background data. This was accomplished in Matlab by using Otsu's method on the summation of corresponding FAD and NADH images. Redox ratios were calculated and the binary masks were applied to the resulting images.

The average values of both redox and FLIM were calculated by dividing the summation of pixel values in masked images by the total number of nonzero pixels in the masks created for each field of view. Fields of view for each mouse were averaged into a single value and used for statistical analysis.

2.5 *Statistical methods*

JMP Pro 13 was used for all statistical testing. Kruskal-Wallis test was used when comparing more than two groups, and Wilcoxon exact test (Wilcoxon test) was used to test the differences between and within cell lines. When testing within cell lines mice were used as the blocking variable to account for inter-subject variability and subjects with missing data for an oxygen condition were excluded. Level of significance was considered $p<0.05$ for all tests.

3. Results

3.1 *Twist expression and exposure to hypoxia affects vascular oxygenation within the early tumor*

Hyperspectral imaging was used to determine the vascular oxygenation and total hemoglobin concentration within the early tumor. This served two purposes. First, it couldn't be assumed that exposure to one hour of hypoxia would cause a shift in oxygen availability within the tumor. It may be possible for breathing rate and heart rate to affect systemic oxygen levels. If hypoxia is compensated for by the mouse hypoxic perturbations would not necessarily affect oxygen availability within the tumor. Hyperspectral imaging allows us to quantify changes in vascular oxygenation. Second, we sought to determine if Twist expression had an effect on vascular oxygenation. Twist could potentially affect vascular oxygenation by affecting angiogenesis or by altering metabolism.[38]If Twist led to an increase in OXPHOS oxygen consumption would increase and this would result in a decrease of vascular oxygenation. The opposite would be expected for an increase in glycolysis- assuming this requires a decrease in OXPHOS. Pseudo-colored, vascular oxygenation images were created from hyperspectral imaging data. Representative images of vascular oxygenation can be seen in Figure 1. The magenta lines in the normoxia images represent the regions of interest that encompass the area of the tumors and exclude tissue which appears normal. Histograms of vascular oxygenation

are also in Figure 1. These histograms are the average vascular oxygenation for all images in each group. In the representative images the drop in oxygenation within the tumor can be seen by the slight shift towards blue in the blood vessels. During reperfusion there appears to be a hyperemic response as the redshift extends beyond what was seen under normoxia. This is supported by the histograms where the average percent of pixels is plotted with percent of

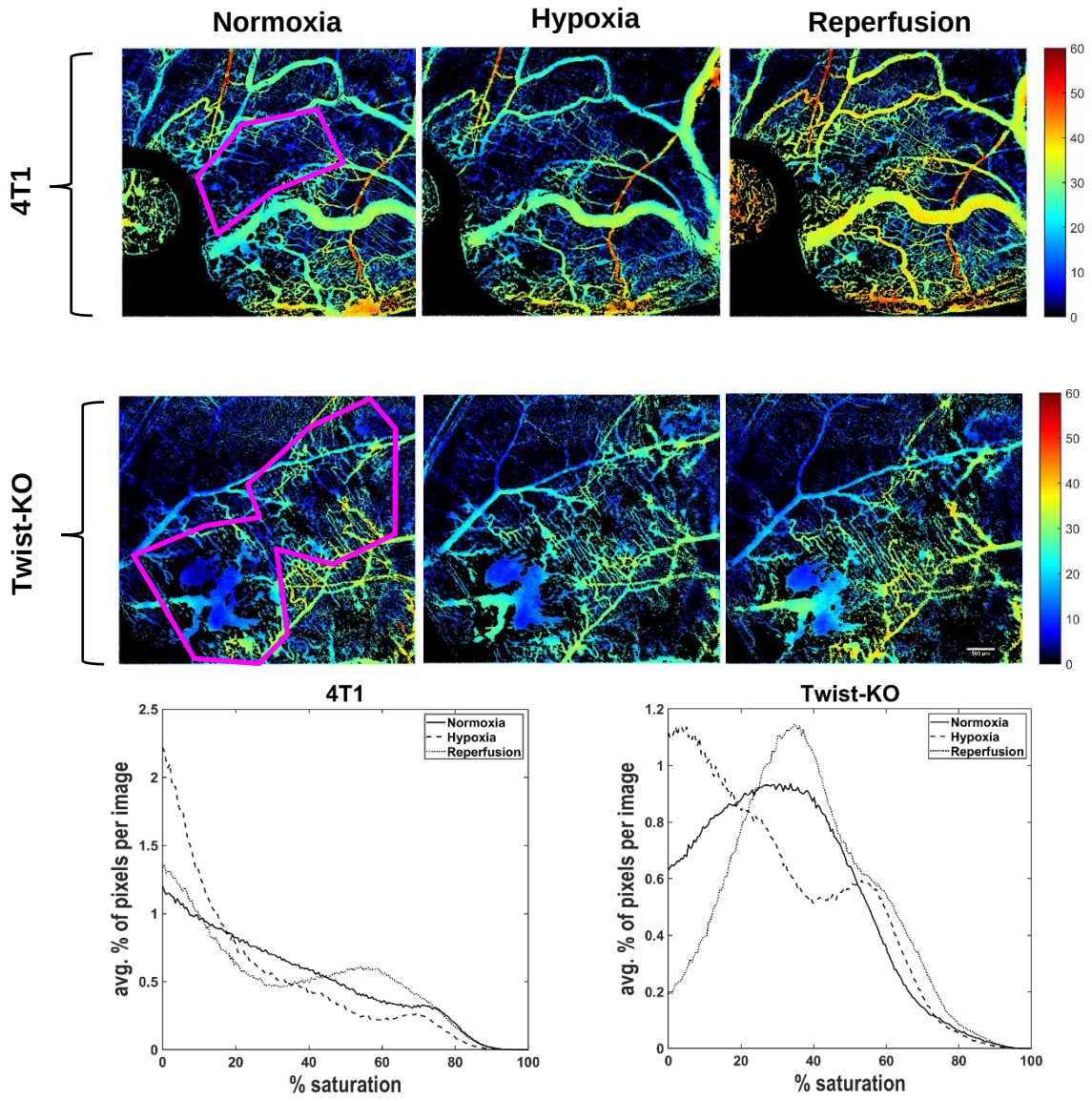

Figure 1: First and second rows are pseudo-colored hyperspectral images of 4T1 and Twist-KO tumors under normoxia, hypoxia, and reperfusion. Magenta lines are representative of the regions of interest that are comprised of tumors. Bottom row consists of histograms representing the average percent of pixels corresponding to oxygen saturation of hemoglobin within vasculature of tumors for normoxia, hypoxia, and reperfusion.

vascular oxygenation where zero percent would represent blood vessels where no hemoglobin is bound to oxygen. Looking at the peaks and shapes of the plotted histograms a clear shift to the less oxygen-hemoglobin binding is seen during hypoxia, and under reperfusion it seems to shift the other way and goes slightly beyond normoxia. This qualitatively shows that hypoxia perturbation is altering oxygen availability as expected.

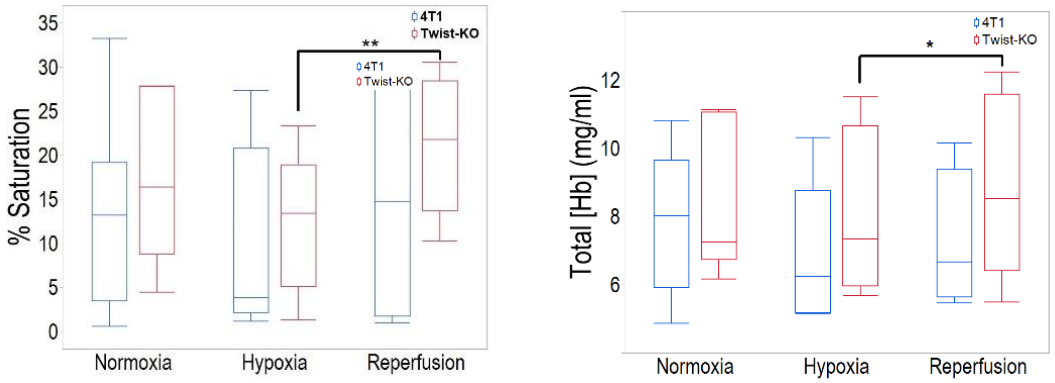

Figure 2: Plots are based on the mean values of vascular oxygenation and total hemoglobin concentration. For 4T1 sample sized varied (normoxia n=8: hypoxia n=5: reperfusion n=4). For Twist-KO n=7 for all oxygen conditions. Statistical significane was determined by Wilcoxon test. (*p<0.05, **p<0.01).

The mean value of the vascular oxygenation and total hemoglobin concentration within the tumor were determined for each mouse and compared by Wilcoxon's test. Results are shown in Figure 2. Vascular oxygenation changes in response to the hypoxia and reperfusion as expected. Total hemoglobin concentration follows a similar trend. In both vascular oxygenation and total hemoglobin concentration the only statistically significant difference is between Twist-KO during hypoxia and reperfusion. No difference was found between the two cell lines, even though it appears 4T1 may generally have lower values.

Furthermore, the changes in vascular oxygenation and total hemoglobin were determined by finding the difference in corresponding hypoxia and normoxia values as well as reperfusion and hypoxia values. Figure 3 shows the change in vascular oxygenation and total

hemoglobin concentration as mice were exposed to hypoxia and allowed to recover. No significant difference was found between cell lines. Within cell lines Twist-KO showed a difference between the shifts in oxygen. It was expected that significant difference would be seen in both cell lines. If not an effect of sample size (n=4) the little amount of change seen in 4T1 may be due to vasculature organization since 4T1 tumors tend to have lower vascular oxygenation and hemoglobin concentration under all oxygen condition.

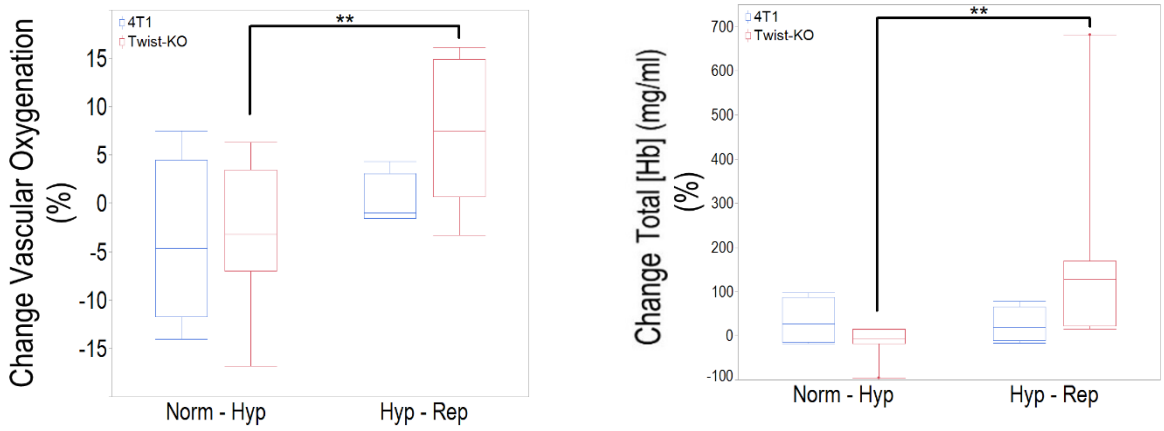

Figure 3: change in vascular oxygenation (left) and change in total hemoglobin concentration (right). (**p<0.01)

3.2 Optical Redox Ratio indicates increased glycolysis in response to oxygen reperfusion for Twist knockout tumors. *A difference in the optical redox ratio is seen between 4T1 and Twist-KO during reperfusion*

The optical redox ratio was determined by multiphoton microscopy to study the effects of Twist on metabolism. Hypoxia was used to perturb the cells and images were acquired at normoxia and reperfusion. Figure 4 shows representative ORR images for 4T1 and Twist-KO under normoxia and reperfusion. The mean ORR for each mouse is represented in figure 5. ORR was significantly different under reperfusion. During reperfusion the ORR of 4T1 increased slightly and the ORR of Twist-KO decreased slightly. This indicates that 4T1 became slightly

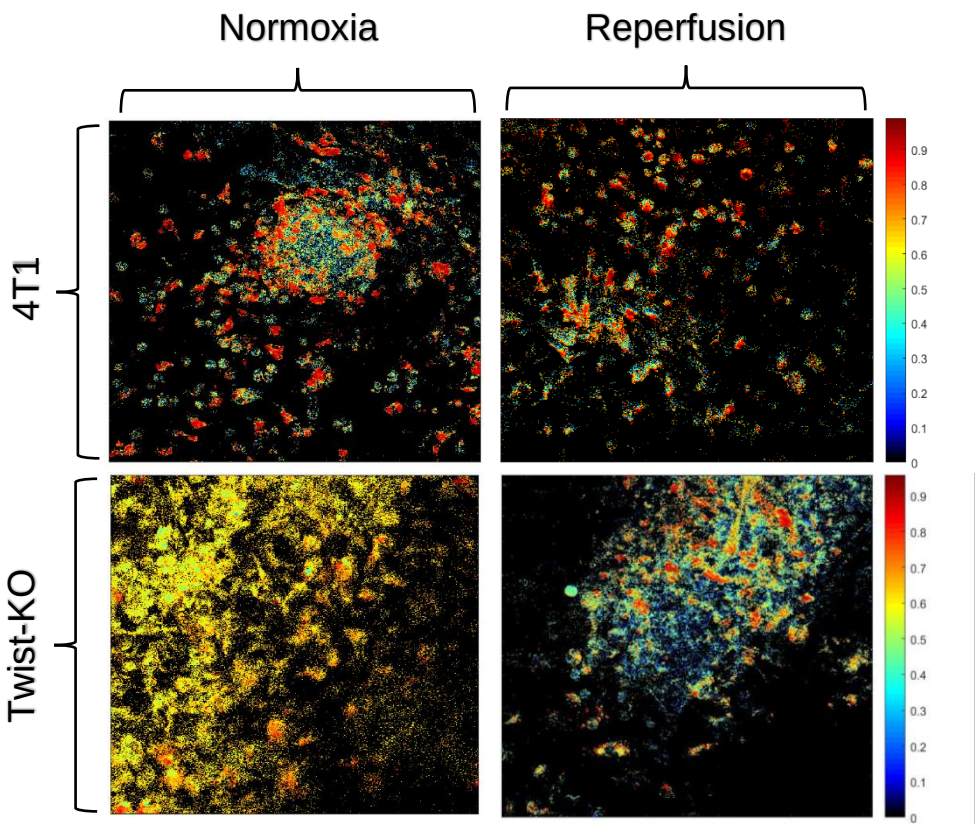

Figure 4: Representative images of the optical redox ratio for 4T1 and Twist under normoxia and reperfusion.

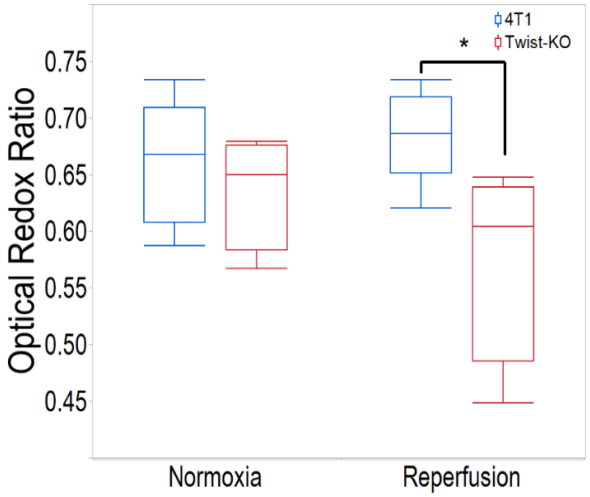

Figure 5: Optical redox ratio for 4T1 and Twist-ko under Normoxia and Reperfusion. Significant difference between the two cell lines under reperfusion. (*p<0.05)

more oxidative when more oxygen was available during reperfusion. The opposite happened in Twist-KO. Although there was more oxygen available during reperfusion than normoxia the ORR decreased, and Twist-KO had become more glycolytic than the Twist overexpressing 4T1 cell line. It is likely that Twist-KO became more glycolytic during hypoxia but could not make the shift back to OXPHOS during the 1 hour of reperfusion. The observed difference between 4T1 and Twist-KO is consistent with previous *in vitro* studies that show a similar correlation between Twist expression and oxygen consumption rate after reperfusion.[19]

3.3 *FLIM indicates no change in NADH binding in response to oxygen reperfusion or Twist expression*

The relative contribution of free to bound NADH is another measure of the relative use of glycolysis and OXPHOS and is the primary data from FLIM used in this study. During glycolysis NADH will bind to proteins less often due to the decrease of mitochondrial activity which leads to an increase in free NADH and should cause an increase in the A1/A2 ratio. Representative images of A1/A2 ratio can be seen in figure 6.

In fig. 5 the ORR of Twist-KO appeared to decrease; however, no change was detected in the A1/A2 ratio as seen in Figure 7. The decreased ORR for Twist-KO would lead us to believe that the A1/A2 ratio should increase in Twist-KO. Whether this didn't happen due to small sample sizes, fluorescence of other metabolites, or experimental error is unknown Similarly, the lifetime of free and bound NADH as seen in Figure 7 is not as expected. There was no difference in lifetime between the oxygen conditions for either cell line; however, there was drastic differences between cell lines. Note that the lifetime of free NADH (tau 1) should only change minimally between these two cell lines. This was not case, and a large difference in tau 1 and tau 2 were observed. This is very likely due to experimental error since lifetime changed drastically between two experiments.

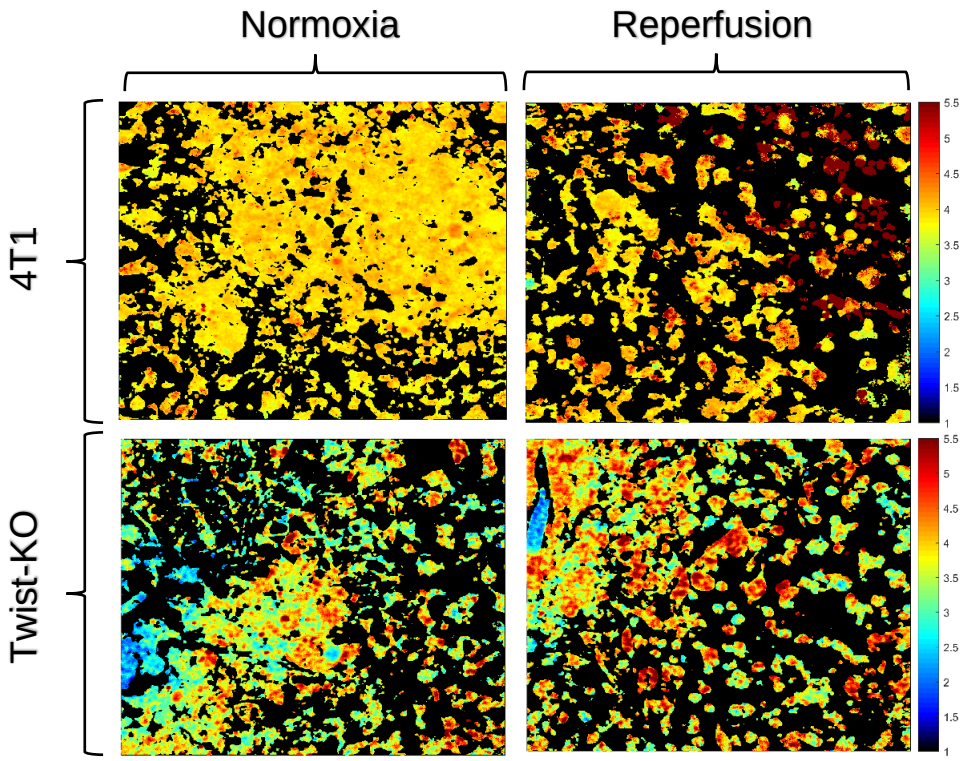

Figure 6: Representative images of A1/A2. A1/A2 ratio shows no significant difference within or between cell lines. N=3 and n=4 for 4T1 and Twist-KO respectively.

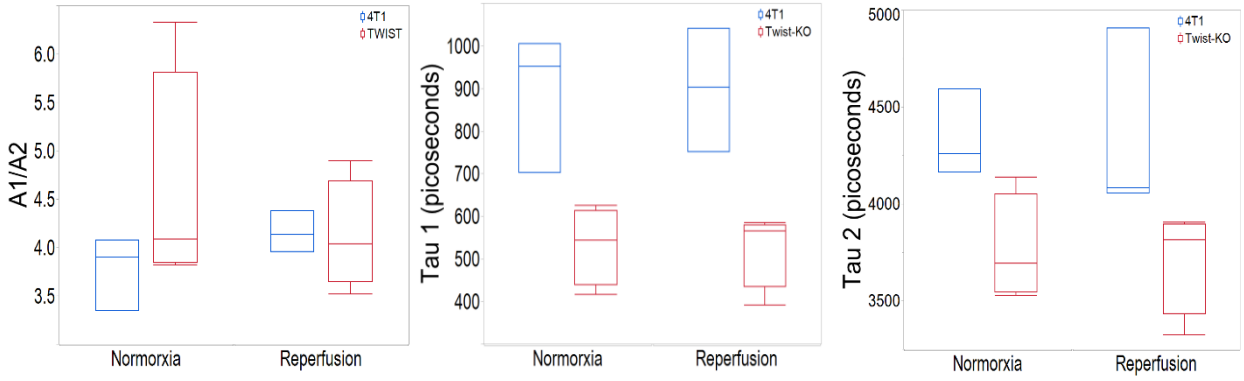

Figure 7: Lifetimes are not different within cell lines. There are clear differences between cell lines; however, these may be due to experimental error.

Additionally, there was no apparent relationship between lifetime and redox ratio (Table 1). As cells become more glycolytic the redox ratio is expected to decrease while the relative contribution of free to bound NADH is expected to increase.

Table 1: Median values for redox ratio and FLIM. The two imaging modalities showed no discernable congruence.

	REDOX		FLIM	
	Normoxia	**Reperfusion**	**Normoxia**	**Reperfusion**
4T1	0.671227	0.69089576	3.893641	4.103821
TWIST-KO	0.67605	0.619365207	4.19843	4.116843

4. Discussion

Twist, although necessary in early development, has been associated with poor prognosis when overexpressed in cancers.[35] This may be due to Twist's association with EMT and EMR, both of which have been associated with tumor invasion, survival, and metastasis.[3,7,8,39] Previous studies in our lab have explored the cellular metabolic response to hypoxia perturbation.[15,19] These studies found that the Twist overexpressing cell line 4T1 retained its glycolytic nature after hypoxic recovery while Twist-KO transitioned to a more glycolytic metabolism. These experiments were done *in vitro*. Although an important first step, it is critical for these findings to be tested *in vivo.*[35] The tumor microenvironment is more complex than the cell cultures can model and introduces variables that are present only in living tissue.

It was necessary to determine the oxygen saturation within the tumor microenvironment because hypoxia was induced by exposing mice to a low oxygen environment rather than directly controlling the oxygen availability to the cells as is done *in vitro*. Hyperspectral imaging was used to quantify change in oxygen saturation in response to the hypoxic exposure to study the effect of Twist on oxygen availability within the tumor vasculature. The general change in vascular oxygenation that is expected in response to hypoxia and reperfusion were seen; oxygen availability decreased under hypoxia and then increased to higher than normal levels during reperfusion. However, quantitatively the change was only significant between hypoxia

and reperfusion within the Twist-KO cell line. This change was also expected in 4T1. The decreased ORR of Twist-KO after hypoxia may be responsible for the increased oxygen availability. If cells decrease their use of OXPHOS it is possible that they are also decreasing their uptake of oxygen. A decreased uptake of oxygen would lead to higher vascular oxygenation as seen in fig. 2 and fig. 3. Determining correlation of vascular and metabolic changes could be improved with a more consistent method for tumor area selection. In this experiment vascular imaging and metabolic imaging were performed with two different microscopes using different magnifications. When performing hyperspectral imaging the tumor area can be clearly seen and the images acquired are of a large area of the tumor- sometimes the entire tumor area. However, in multiphoton imaging the magnification is much higher and the border of the tumor is not clearly defined. This problem could be solved by tagging cells with red fluorescent protein or by combining imaging modalities on one platform. Tagging cells with red fluorescent protein would allow cancer cells to be easily distinguished from the surrounding normal cells in multiphoton imaging. Combining imaging modalities to one platform would help in acquiring images for all modalities in the same region. If imaging modalities were combined to one platform hyperspectral and fluorescent images could be consistently acquired from the same region.

The ORR of 4T1 *in vitro* was shown in a previous study to increase during reperfusion.[15] In this *in vivo* study we saw the ORR of 4T1 remain relatively unchanged. Whether this is due to the time points that ORR is being measured at or differences between *in vivo* and *in vitro* conditions remains unknown. However, the ORR of Twist-KO decreased significantly during reperfusion. The lowered ORR after reperfusion is seen in Twist-KO, but not 4T1. This may indicate that Twist expression allows 4T1 to recover from hypoxia more quickly than Twist-KO or it may inhibit the response to hypoxia in 4T1 that is seen in Twist-KO. To better understand

how Twist expression affects the response to hypoxia and reperfusion a set of subjects should be measured during hypoxia.

Although the ORR changed significantly the A1/A2 ratio did not. This could be due to small sample size used for FLIM (n=3 4T1 and n=4 Twist-KO) or it could be caused by the unexpected shift in lifetime that occurred. If not due to small sample size or experimental error, it could be caused by metabolic pathways such as the pentose phosphate pathway (PPP) which utilizes NADPH. NADH and NADPH are used in distinctly different metabolic pathways.[40] However, the fluorescence spectra of NADH and NADPH overlap making it difficult to separate the two.[41,42] If usage of metabolic pathways such as the PPP were increased it is possible that this would affect the lifetime data. These potential sources of variation may also be why there was no discernable congruence between lifetime and redox data.

It was particularly interesting that the lifetimes had more variation between cell lines than the A1/A2 ratio. The A1/A2 ratio remained fairly similar, but the lifetime was abnormally long in the 4T1 cells.[29,30,37,41] This is likely error since the lifetime of free NADH changed drastically as well. Lifetime is known to be affected by environmental factors such as pH, temperature, and other fluorescent quenchers.[29,43,44] Oxygen concentration, temperature, and pH would be the most likely confounding variables in this case. Oxygen saturation was measured but no differences were seen between cell lines or between the time points used for FLIM in this experiment. Temperature is a potential problem since the window chamber holds a thin layer of skin away from the body where it may cool or heat more rapidly than if it were in good contact with the rest of the body. Although the heating pad used for the mice did not measure internal body temperature it is unlikely that heating discrepancies would occur in only the 4T1 or Twist-KO group. Finally, pH could change as a result of metabolic differences, but it is unlikely that the pH difference would be great enough to cause the large differences found in the results.[45]

Additionally, instrument calibration and the researchers are other potential sources of variation. The chance of error caused by either of these could be mitigated in the future. A positive control could be used to determine if the instrument is calibrated correctly and possibly allow for corrections to the data if needed. Imaging a solution of NADH of specified concentration and temperature during each imaging session would be a simple control that would allow for errors in instrument calibration to caught during data analysis.[46] As already discussed, tagging the cancer cells with RFP would assure the correct regions were imaged. This could prevent user bias and misidentification of nontumor areas as the regions of interest.

In vivo and *in vitro* studies suggest Twist expression alters the metabolic behavior of breast cancer. However, cancer is not a heterogenous disease. The murine breast cancer cell lines used in this study are not necessarily representative of all cancers, and these findings cannot be applied universally. Even within a single tumor there can be multiple genetic subpopulations.[47]

Future studies need to include other breast cancer cell lines, and if findings are consistent the study could be expanded to cancers originating in other tissues. Also, the ORR and A1/A2 ratio were looked at only under normoxia and reperfusion; the next step is to expand the protocol to include imaging during hypoxia as was done with hyperspectral imaging. This is needed to determine if changes observed in Twist-KO are occurring during hypoxia or reperfusion.

In conclusion, Twist transcription factor does affect metabolism *in vivo*; however, further studies are needed to determine the mechanism of Twist's influence. A noticeable difference in the metabolic response to re-oxygenation following acute hypoxia is seen between the 4T1 cell line and the Twist deleted cell line. Their ORRs are similar under normoxia, but Twist-KO has decreased ORR following reperfusion indicating increased glycolysis while 4T1 remains

unchanged. The metabolic change in Twist-KO is accompanied by increased vascular oxygenation. The oxygen availability in Twist-KO during reperfusion may indicate that the cells are primarily using glycolysis and are not consuming the oxygen. These results show Twist alters the metabolism of the 4T1 cells. This may be done by either increasing the rate at which 4T1 cells switch from glycolysis to OXPHOS or it prevents the switch to glycolysis during hypoxia.

5. References

1. Warburg, O., Wind, F. & Negelein, E. THE METABOLISM OF TUMORS IN THE BODY. *J. Gen. Physiol.* (1927).
2. Chambers, A. F., Groom, A. C. & MacDonald, I. C. Dissemination and growth of cancer cells in metastatic sites. *Nat. Rev. Cancer* **2**, 563–572 (2002).
3. Yang, J. *et al.* Twist, a master regulator of morphogenesis, plays an essential role in tumor metastasis. *Cell* **117**, 927–939 (2004).
4. Yang, M. H. *et al.* Direct regulation of TWIST by HIF-1α promotes metastasis. *Nat. Cell Biol.* (2008). doi:10.1038/ncb1691
5. Kang, Y. & Massague, J. Kang&Massague EMT 2004. **118**, 1–3 (2004).
6. Montserrat, N. *et al.* Repression of E-cadherin by SNAIL, ZEB1, and TWIST in invasive ductal carcinomas of the breast: A cooperative effort? *Hum. Pathol.* **42**, 103–110 (2011).
7. Yang, L. *et al. Twist promotes reprogramming of glucose metabolism in breast cancer cells through PI3K/AKT and p53 signaling pathways*. *Oncotarget* **6**,
8. Porporato, P. E. *et al.* A mitochondrial switch promotes tumor metastasis. *Cell Rep.* (2014). doi:10.1016/j.celrep.2014.06.043
9. Otto Warburg, B., Wind, F. & Negelein, N. THE METABOLISM OF TUMORS IN THE BODY. *J. Gen. Physiol.* (1927). doi:10.1085/jgp.8.6.519
10. Hanahan, D. & Weinberg, R. A. Hallmarks of cancer: the next generation. *Cell* (2011). doi:10.1016/j.cell.2011.02.013
11. Pfeiffer, T. ;, Schuster, S. ; & Bonhoeffer, S. *Cooperation and competition in the evolution of ATP-producing pathways*. (2001).
12. Lin Zu, X. & Guppy, M. Breakthroughs and Views Cancer metabolism: facts, fantasy, and fiction q. doi:10.1016/j.bbrc.2003.11.136
13. Lunt, S. Y. & Vander Heiden, M. G. Aerobic Glycolysis: Meeting the Metabolic Requirements of Cell Proliferation. *Annu. Rev. Cell Dev. Biol* **27**, 441–464 (2011).
14. Lu, X., Bennet, B., Mu, E., Rabinowitz, J. & Kang, Y. Metabolomic Changes Accompanying Transformation and Acquisition of Metastatic Potential in a Syngeneic Mouse Mammary Tumor Model * □ S. (2010). doi:10.1074/jbc.C110.104448
15. Alhallak, K., Rebello, L. G., Muldoon, T. J., Quinn, K. P. & Rajaram, N. Optical redox ratio identifies metastatic potential-dependent changes in breast cancer cell metabolism. *Biomed. Opt. Express* **7**, 4364 (2016).
16. Lebleu, V. S. *et al.* PGC-1α mediates mitochondrial biogenesis and oxidative phosphorylation to promote metastasis migratory/invasive cancer cells specifically favor mitochondrial respiration and increased ATP production. Invasive cancer cells use transcription co-activator, PGC-1α to enhance oxidative HHS Public Access. *Nat Cell Biol* **16**, 992–1007 (2014).
17. Dupuy, F. *et al.* PDK1-dependent metabolic reprogramming dictates metastatic potential in breast cancer. *Cell Metab.* (2015). doi:10.1016/j.cmet.2015.08.007

18. Martin, T. A., Goyal, A., Watkins, G. & Jiang, W. G. Expression of the transcription factors snail, slug, and twist and their clinical significance in human breast cancer. *Ann. Surg. Oncol.* (2005). doi:10.1245/ASO.2005.04.010

19. Harper, M. *et al.* Optical Metabolic Imaging of TWIST Inhibition in 4T1 Breast Cancer Cells. **2017**, OmS2D.3 (2017).

20. Pasqualini, R., Arap, W. & McDonald, D. M. Probing the structural and molecular diversity of tumor vasculature. *Trends in Molecular Medicine* (2002). doi:10.1016/S1471-4914(02)02429-2

21. Palmer, G. M. *et al.* In vivo optical molecular imaging and analysis in mice using dorsal window chamber models applied to hypoxia, vasculature and fluorescent reporters. *Nat. Protoc.* **6**, (2011).

22. Skala, M. C., Fontanella, A., Lan, L., Izatt, J. A. & Dewhirst, M. W. Longitudinal optical imaging of tumor metabolism and hemodynamics. *J. Biomed. Opt.* (2010). doi:10.1117/1.3285584

23. Im, J. & Rajaram, N. Optical Molecular Imaging and Spectroscopy of Oxygenation and Metabolism in Tumors. *IEEE J. Sel. Top. Quantum Electron.* **22**, 78–87 (2016).

24. Rajaram, N., Frees, A. E., Fontanella, A. N., Zhong, J. & Hansen, K. Delivery Rate Affects Uptake of a Fluorescent Glucose Analog in Murine Metastatic Breast Cancer. *PLoS One* **8**, 76524 (2013).

25. Sorg, B. S., Moeller, B. J., Donovan, O., Cao, Y. & Dewhirst, M. W. Hyperspectral imaging of hemoglobin saturation in tumor microvasculature and tumor hypoxia development. *J. Biomed. Opt.* **10**, 044004 (2005).

26. Chance, B., Schoener, B., Oshino, R. & Itshak, F. Oxidation-Reduction Ratio Studies of Mitochondria in Freeze-trapped. **254**, (2013).

27. Quinn, K. P. *et al.* Quantitative metabolic imaging using endogenous fluorescence to detect stem cell differentiation. *Sci. Rep.* (2013). doi:10.1038/srep03432

28. Hou, J. *et al.* Correlating two-photon excited fluorescence imaging of breast cancer cellular redox state with seahorse flux analysis of normalized cellular oxygen consumption. *J. Biomed. Opt.* **21**, 060503 (2016).

29. Skala, M. C. *et al.* In vivo multiphoton fluorescence lifetime imaging of protein-bound and free nicotinamide adenine dinucleotide in normal and precancerous epithelia. *J. Biomed. Opt.* (2007). doi:10.1117/1.2717503

30. Li, D., Zheng, W. & Qu, J. Y. Time-resolved spectroscopic imaging reveals the fundamentals of cellular NADH fluorescence. *Opt. Lett.* (2008). doi:10.1364/ol.33.002365

31. Suhling, K., French, P. M. W. & Phillips, D. Time-resolved fluorescence microscopy. *Photochem. Photobiol. Sci.* (2005). doi:10.1039/b412924p

32. Sharick, J. T. *et al.* Protein-bound NAD(P)H Lifetime is Sensitive to Multiple Fates of Glucose Carbon. *Sci. Rep.* (2018). doi:10.1038/s41598-018-23691-x

33. Stringari, C., Nourse, J. L., Flanagan, L. A. & Gratton, E. Phasor Fluorescence Lifetime Microscopy of Free and Protein-Bound NADH Reveals Neural Stem Cell Differentiation Potential. *PLoS One* (2012). doi:10.1371/journal.pone.0048014

34. Stringari, C. *et al.* Metabolic trajectory of cellular differentiation in small intestine by Phasor Fluorescence Lifetime Microscopy of NADH. *Sci. Rep.* (2012). doi:10.1038/srep00568

35. Neveu, M. A. *et al.* Multimodality Imaging Identifies Distinct Metabolic Profiles In Vitro and In Vivo. *Neoplasia (United States)* (2016). doi:10.1016/j.neo.2016.10.010

36. Lu, G. & Fei, B. Medical hyperspectral imaging: a review. doi:10.1117/1.JBO.19.1.010901

37. Jones, J. D., Ramser, H. E., Woessner, A. E. & Quinn, K. P. In vivo multiphoton microscopy detects longitudinal metabolic changes associated with delayed skin wound healing. *email kyle@quinnlab.org) Commun. Biol.* | **1**, (2018).

38. Mironchik, Y. *et al.* Twist overexpression induces in vivo angiogenesis and correlates with chromosomal instability in breast cancer. *Cancer Res.* **65**, 10801–10809 (2005).

39. Thiery, J. P., Acloque, H., Huang, R. Y. J. & Nieto, M. A. Epithelial-mesenchymal transitions in development and disease. *Cell* (2009). doi:10.1016/j.cell.2009.11.007

40. Jiang, P., Du, W. & Wu, M. Regulation of the pentose phosphate pathway in cancer. *Protein Cell* (2014). doi:10.1007/s13238-014-0082-8

41. Blacker, T. S. *et al.* Separating NADH and NADPH fluorescence in live cells and tissues using FLIM. *Nat. Commun.* (2014). doi:10.1038/ncomms4936

42. Rocheleau, J. V., Head, W. S. & Piston, D. W. Quantitative NAD(P)H/flavoprotein autofluorescence imaging reveals metabolic mechanisms of pancreatic islet pyruvate response. *J. Biol. Chem.* **279**, 31780–31787 (2004).

43. Berezin, M. Y. & Achilefu, S. Fluorescence Lifetime Measurements and Biological Imaging. doi:10.1021/cr900343z

44. Suhling, K., French, P. M. W. & Phillips, D. Time-resolved fluorescence microscopy. *Photochem. Photobiol. Sci.* **4**, 13–22 (2005).

45. Islam, M., Honma, M., Nakabayashi, T., Kinjo, M. & Ohta, N. pH Dependence of the Fluorescence Lifetime of FAD in Solution and in Cells. *Int. J. Mol. Sci.* **14**, 1952–1963 (2013).

46. Lakowicz, J. R., Szmacinski, H., Nowaczyk, K. & Johnson, M. L. *Fluorescence lifetime imaging of free and protein-bound NADH*. *Biochemistry* **89**, (1992).

47. Fisher, R., Pusztai, L. & Swanton, C. Cancer heterogeneity: implications for targeted therapeutics. (2013). doi:10.1038/bjc.2012.581

6 Appendices

6.1 Appendix A: IACUC Protocol Approval #18062

UNIVERSITY OF ARKANSAS

Office of Research Compliance

To:	Narasimhan Rajaram
Fr:	Craig Coon
Date:	January 17th, 2018
Subject:	IACUC Approval
Expiration Date:	December 19th, 2018

The Institutional Animal Care and Use Committee (IACUC) has APPROVED your protocol # **18062:** *Intravital microscopy of tumor oxygenation and metabolism in metastatic and non-metastatic breast cancers.*

In granting its approval, the IACUC has approved only the information provided. Should there be any further changes to the protocol during the research, please notify the IACUC in writing (via the Modification form) prior to initiating the changes. If the study period is expected to extend beyond December 19th, 2018, you can submit a modification to extend project up to 3 years, or submit a new protocol. By policy the IACUC cannot approve a study for more than 3 years at a time.

The following individuals are approved to work on this study: Narasimhan Rajaram, Sina Dadgar, Joel Rodriguez Tron, Paolo Monterroso-Dia, and Brandon Sturgill. Please submit personnel additions to this protocol via the modification form prior to their start of work.

The IACUC appreciates your cooperation in complying with University and Federal guidelines involving animal subjects.

CNC/tmp

18062

6.2 Appendix B: Supplementary Images

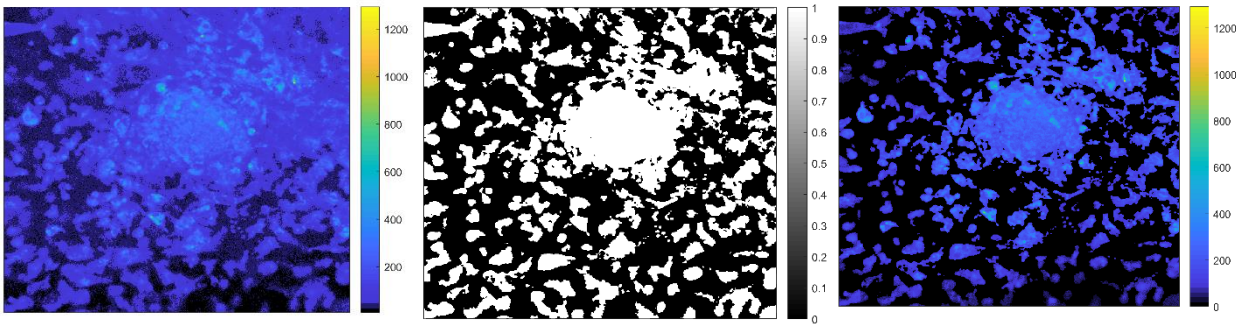

Figure S1: Masks are based on the intensity image and are then applied to redox images and FLIM images. Fluorescent lifetime Intensity image at the far left was used to create the binary mask in the center. On the far right is the intensity image with mask applied.